Activation of caspase-1 by the NLRP3 inflammasome regulates the NADPH oxidase NOX2 to control phagosome function

Published in final edited form as:
Nat Immunol. 2013 June ; 14(6): 543–553. doi:10.1038/ni.2595.

Activation of caspase-1 by the NLRP3 inflammasome regulates the NADPH oxidase NOX2 to control phagosome function

Anna Sokolovska[1,*,†], **Christine E. Becker**[1,*], **WK Eddie Ip**[1,#], **Vijay A.K. Rathinam**[2], **Matthew Brudner**[1], **Nicholas Paquette**[1], **Antoine Tanne**[1], **Sivapriya K. Vanaja**[2], **Kathryn J. Moore**[3], **Katherine A. Fitzgerald**[2], **Adam Lacy-Hulbert**[1], and **Lynda M. Stuart**[1,4,†]

[1]Developmental Immunology/CCIB, Massachusetts General Hospital/Harvard Medical School, Boston, MA 02114, USA.

[2]Division of Infectious Diseases and Immunology, Department of Medicine, University of Massachusetts Medical School, Worcester, MA, USA.

[3]Departments of Medicine and Cell Biology, New York University Medical Center, New York, USA.

[4]The Broad Institute of Harvard and MIT, Cambridge, MA 02142.

Abstract

Phagocytosis is a fundamental cellular process that is pivotal for immunity as it coordinates microbial killing, innate immune activation and antigen presentation. An essential step in this process is phagosome acidification, which regulates a number of functions of these organelles that allow them to participate in processes essential to both innate and adaptive immunity. Here we report that acidification of phagosomes containing Gram-positive bacteria is regulated by the NLRP3-inflammasome and caspase-1. Active caspase-1 accumulates on phagosomes and acts locally to control the pH by modulating buffering by the NADPH oxidase NOX2. These data provide insight into a mechanism by which innate immune signals can modify cellular defenses and establish a new function for the NLRP3-inflammasome and caspase-1 in host defense.

A particularly important process in host defense is phagocytosis, the internalization of particles into organelles called ‘phagosomes’ that restrict microbial replication and participate in the presentation of antigens to prime T cell responses [1]. Despite this crucial role in immunity, the molecular mechanisms that regulate the functions of phagosomes remain poorly understood. What is known is that phagosomes in macrophages are dynamically remodelled during their ‘maturation’ by the sequential fission with early and then late endosomes, and ultimately fusion with lysosomes [2-4]. An important aspect of the maturation process is vacuolar acidification, which regulates the activity of the pH-sensitive enzymes that are delivered from lysosomes and required to digest internalized cargo [5]. The

[†]Address correspondence to: Lynda Stuart or Anna Sokolovska Developmental Immunology Jackson14, Massachusetts General Hospital/Harvard Medical School 55 Fruit Street Boston, MA 02114 Tel 617-724-2890 Fax 617-724-3248 lstuart@partners.org or asokolovska@partners.org.
[#]Current Address: Department of Immunobiology Yale School of Medicine 300 Cedar Street New Haven, CT
[*]These authors contributed equally to this work

To obtain full methods and protocols please contact manuscript authors.

AUTHOR CONTRIBUTIONS A.S., C.B. and W.K.I.P designed, analyzed and performed experiments. V.R, M.B., N.P., A.T., and S.V. contributed to experimental design, provided discussions and assisted with experiments. K.M, K.F and A.L-H contributed to data analysis, discussions and manuscript preparation. L.S. designed, analyzed, supervised the project and prepared the manuscript with A.S. and C.B.

COMPETING FINANCIAL INTERESTS The authors declare no competing financial interests.

timely delivery of microbes into a mature and acidified phagolysosome is essential not only for microbial killing [6], but also to facilitate activation of certain innate immune signalling pathways [7]. Moreover, the rate of phagosome acidification also regulates antigen processing and presentation by macrophages and dendritic cells (DCs) [8]. Because of these pivotal roles in immunity, understanding the mechanisms that allow the host to remodel phagosomal compartments to optimize their microbicidal and hydrolytic activity is of fundamental importance.

Acidification is key to many facets of phagosome function. It is a regulated process that begins almost immediately after the phagocytic cup has closed [9,10] and, for certain cargo, the luminal pH can drop from 7 to 4 in a matter of minutes. These rapid changes precede the fusion with acidic compartments and instead early acidification requires delivery of the vacuolar-H^+-ATPase (V-ATPase)[11]. This proton transporting holoenzyme is recruited from endosomes and lysosomes, and assembled on the membrane of the nascent vacuole [9,12]. However, how the pH is then regulated remains poorly defined. V-ATPase activity in mammalian macrophages and DCs can be 'primed' by innate immune stimuli, through a process that appears to require transcriptional regulation [13,14]. Additionally, the NADPH oxidase has been suggested to counteract the V-ATPase and neutralize the phagosome pH in certain cells [15]. A number of pathogens have evolved mechanisms to evade these processes, including buffering their local environment in an attempt to maintain a beneficial neutral pH.

The nature of the mature phagosome is therefore determined by the complex interplay between the internalized microbe and the rapid remodeling of the organelle by the host in response to the different cargo. The observation that Toll-like receptors (TLRs) are recruited to some phagosomes [16-18] led to the proposal that phagosome-associated TLRs might survey the luminal contents and control vacuole maturation in a cargo-dependent and organelle autonomous manner to mediate these rapid changes[19,20]. Although attractive as a mechanism for sensing and remodeling the phagosome depending on the type of internalized material, this function of the TLRs remains controversial, especially as the molecular details of how they might regulate this process remains obscure [20]. The rapidity of the changes that occur after microbial engulfment argues against the fate of the phagosome being controlled at a transcriptional level. Rather we reasoned that local, post-translational modifications induced by innate immune signals were more likely to underlie the prompt remodeling of the phagosome that occurs after internalization of different microbes. To investigate this possibility, we chose to focus on the inflammasome, as it is an innate immune pathway whose terminal effectors are proteases that can rapidly modify select host components. We found that caspase-1 is rapidly activated upon phagocytosis of Gram-positive microbes. Moreover, we demonstrate that activation of the NLRP3 inflammasome and its effector, caspase-1, are instrumental in enabling the microbicidal activity of *Staphylococcus aureus*-containing phagosomes. Caspase-1 acts on the NADPH oxidase (NOX2), and by controlling its activity it modifies the pH of the vacuole. These findings identify an essential role of caspase-1 in locally coordinating the environment of phagosomes. We propose that this cell autonomous defense function of caspase-1 acts in concert with its role in pro-inflammatory cytokine release and pyroptosis and thus positions it as a master regulator of innate immunity.

Results

Caspase-1 accumulates on phagosomes containing *S. aureus*

Infection with Gram-positive microbes causes assembly of the NLRP3 inflammasome and activation of caspase-1[21]. While investigating inflammasome activation during *S. aureus* phagocytosis we observed that total caspase-1, monitored by using either an anti-caspase-1

antibody in bone marrow derived macrophages (Figure 1a) or by transfection of RFP-caspase-1 into RAW 264.7 cells (Figure 1b), was found not only in the cytosol but was also enriched on phagosomes. Caspase-1 exists as both an inactive pro-enzyme and, after auto-proteolytic cleavage in an inflammasome platform, an active protease. As these methods could not distinguish pro-caspase-1 from active caspase-1 we used the Fluorescent Labelled Inhibitor of Caspases (FLICA) reagent, which forms a covalent bond with the active protease [22], to determine the localization of active caspase-1 (Figure 1c-f). Active caspase-1 accumulated around bacterial phagosomes (Figure 1c). The FLICA staining required internalization of *S. aureus* as it was blocked by cytochalasin D (Figure 1d). The localization of caspase-1 after *S. aureus* phagocytosis contrasted with the widespread cytoplasmic distribution of active caspase-1 seen following treatment with LPS and ATP, a non-particulate activator of the NLRP3 inflammasome (Figure 1e). The accumulation of active caspase-1 on phagosomes was cargo-dependent; latex bead phagosomes did not stain with FLICA, despite the presence of total caspase-1 as detected by antibody staining (Supplementary Fig. 1a-c) and phagocytosis of the Gram-negative bacterium *Escherichia coli* was not associated with detectable caspase-1 activation in unprimed cells (Supplementary Figure 1d,e). Together these data indicate that caspase-1 was activated and then specifically recruited to *S. aureus* phagosomes.

Caspase-1 activation triggered by *S. aureus* phagocytosis

We next sought to better define what regulated caspase-1 activation after *S. aureus* phagocytosis. Activation was dependent on the NLRP3 inflammasome, as cells deficient in *Ice* (caspase-1), or the inflammasome components *Asc* and *Nlrp3* all failed to activate caspase-1 as measured by flow cytometry (Figure 2a). A similar reduction of FLICA staining was observed when confocal microscopy was used to assess both the total FLICA staining and the amount of phagosome-associated active caspase-1 (Figure 2b). These data confirmed that the FLICA staining was specific and indicated that the inflammasome was required for the phagosome-associated caspase-1.

To establish the kinetics of this activation we monitored the generation of mature caspase-1 p10 by immunoblotting (Figure 2c). Although caspase-1 could not be detected in cell supernatants at early time points, we did observe the appearance of caspase-1 p10 in cell lysates as early as 15 minutes after internalization of bacteria (Figure 2c). To further define the kinetics, we used flow cytometry to monitor YVAD-FLICA. Phagocytosis of both live and heat-inactivated (HI) *S. aureus* was associated with early caspase-1 activation (within 15 minutes of internalization) (Figure 2d). Early caspase-1 activation did not require priming initiated by NF-κB as it was not blocked by the inhibitors BAY 11-7085 or QNZ (Figure 2e). Similarly, it did not require TLR signaling as it was unimpaired in *Myd88*$^{-/-}$ *Trif*$^{-/-}$ cells (Figure 2f). Early caspase-1 activation was also not attenuated by Bafilomycin A, an inhibitor of the V-ATPase, indicating that vacuolar acidification did not play a role at this early point (Figure 2g-h). Instead we observed that phagocytosis of *S. aureus* was associated with generation of reactive oxygen species (ROS) (Figure 2g), which contributed to caspase-1 activation as demonstrated by reduced activation in the presence of low dose diphenylene iodonium (DPI), an inhibitor of ROS (Figure 2h). However, and consistent with previous reports, caspase-1 activation was normal in gp91-phox deficient macrophages indicating that the source of the ROS that activates the inflammasome was not the phagocyte oxidase (NOX2) (Supplementary Figure 2a). Notably, addition of DPI, either alone or with Bafilomycin A, did not completely block caspase-1 activation indicating that there are other additional, but currently unidentified factors, that contribute to activate the inflammasome early during phagocytosis. Unlike *S. aureus*, internalization of *E. coli* was associated with minimal ROS (Figure 2i) and negligible early caspase-1 activation (Figure 2j). Further arguing against a role for ROS in early *E. coli* phagocytosis, addition of DPI had no effect

on the small amounts of caspase-1 activation observed with *E. coli* uptake (Figure 2j). Thus phagocytosis triggered ROS and early caspase-1 activation occurs during the uptake of select microbes.

In contrast, late or sustained caspase-1 activation (>1 hour after infection) was observed only with live and not heat killed *S. aureus*, (Figure 2d and Supplementary Figure 2b) suggesting that factors associated with viable bacteria stabilize inflammasome activity, resulting in both increased duration and amplitude of the signal. Consistent with previous reports, *S. aureus* internalization only led to IL-1β release at later time points if the bacteria were both viable and virulent as HI *S. aureus* or the Sar / Agr mutants that fail to express virulence factors did not induce the late caspase-1 and IL-1β release (Supplementary Figure 2b,c). The sustained activation of caspase-1 and IL-1β release required internalization of bacteria because it could be blocked by Cytochalasin D (Figure 2k,l, Supplementary Fig. 2d). Late caspase-1 activation and IL-1β release was also partially dependent on the proton pump and vacuolar acidification as it was attenuated by the addition of Bafilomycin A (Figure 2k,l and Supplementary Figure 2d). Together these data indicate that caspase-1 activation begins immediately after internalization of *S. aureus*, and suggest that early NLRP3 inflammasome activation is triggered by events such as ROS production that are associated with the phagocytic process.

Caspase-1 regulates phagosome pH

To address the physiological relevance of phagocytosis-associated caspase-1 activation we chose to focus on acidification, as this is an important regulator of many functions of phagosomes. The pH of phagosomes containing certain live bacteria including *S. aureus* is actively neutralized by the microbes they contain [23] (Supplementary Fig. 3a), complicating their use to measure phagosome acidification. Therefore we first measured acidification using HI bacteria which are unable to neutralize the phagosome. For this purpose the rate of acidification was monitored using a highly sensitive and accurate ratiometric assay (Figure 3a,b) in cells pretreated with either a pan-caspase (ZVAD) or caspase-1 specific inhibitor (YVAD). Both ZVAD and YVAD inhibited acidification of *S. aureus* containing vacuoles in a dose-dependent manner (Figure 3b). Similar results were observed when pH was measured by quantifying delivery of pHrodo™ *S. aureus* into acidic compartments (Figure 3c). Caspase inhibition reduced phagosome acidification in all macrophages tested including bone marrow-derived macrophages, peritoneal macrophages, and the macrophage cell lines J774.1 and RAW 264.7 (Figure 3d). Additionally, ZVAD also retarded acidification of phagosomes containing live bacteria (Supplementary Figure 3b).

The kinetics of acidification in the absence of caspase-1 (Supplementary Figure 3c,d) suggested that caspase-1 regulated early acidification and hence was unlikely to act by modifying later steps such as phagosome-lysosome fusion. As an alternative, we explored whether caspase-1 might directly regulate the accumulation of protons in *S. aureus* phagosomes. To test this we used a phagosome pH dissipation assay [24,25] (Supplementary Figure 3e). This assay can estimate the dynamic regulation of pH by monitoring the acute changes induced after pharmacological manipulation of macrophages containing phagosomes that have already acidified. As an example, and similar to previous reports using other bacteria [9,24], acute blockade of the V-ATPase with Bafilomycin A resulted in rapid and total dissipation of the phagosome pH (Figure 3e), confirming that the pH of the *S. aureus* phagosome required the activity of the V-ATPase and that this assay was able to measure proton concentration in the phagosome in real-time. Addition of ZVAD (data not shown) and YVAD (Figure 3f) resulted in partial dissipation of the pH of phagosomes containing both live and HI *S. aureus*. The data from these dissipation assays along with the kinetics argue against caspase-1 regulating the fusion of phagosomes with lysosomes, as this would occur later and not be acutely reversible with any treatment. Rather these data suggest

that caspase-1 acts to directly control the rate of accumulation of protons in the lumen of the organelle.

The NLRP3 inflammasome regulates phagosome pH

To better define the upstream events that trigger the early caspase-1 activation that regulates phagosome acidification we used macrophages from mice with targeted deletions of genes in the caspase-1 regulation pathway. Similar to macrophages treated with caspase inhibitors (Figure 3), bone marrow-derived macrophages that lacked caspase-1 ($Ice^{-/-}$) also showed impaired phagosome acidification (Figure 4a). Furthermore, $Nlrp3^{-/-}$ and $Asc^{-/-}$ bone marrow-derived macrophages showed impaired phagosome acidification (Figure 4b,c), confirming that the NLRP3 inflammasome was upstream of caspase-1 in this context. In contrast, macrophages from 129P3/J and 129x1/SvJ mice that lack caspase-11 showed no defect in phagosome acidification (Figure 4d) excluding any potential involvement of caspase-11, which is also deficient in $Ice^{-/-}$ mice. This defect in acidification was specific for *S. aureus* and not *E. coli* as these phagosomes acidified normally in $Ice^{-/-}$, $Nlrp3^{-/-}$ and $Asc^{-/-}$ cells (Figure 4e,f). These data also confirmed that there was no global abnormality in the endolysosome compartment of inflammasome deficient cells.

As previous work has implicated TLRs in regulating phagosome maturation we also tested if TLRs were required for acidification. $Tlr2^{-/-}$ *and* $Myd88^{-/-}$ macrophages not only phagocytosed *S. aureus* normally, but also acidified *S. aureus*-containing phagosomes with kinetics comparable to that of WT cells (Figure 4g). Similarly, neither TLR adaptors TRIF and Myd88 were required as no defect in acidification was observed in the $Trif^{-/-}$ $Myd88^{-/-}$ cells (Figure 4h) nor did TLR priming accelerate acidification (Supplementary Figure 4). These data indicate that TLRs do not play a role in regulating this process and militate against the retarded acidification being due to loss of the autocrine action of IL-1β as Myd88 is the common adaptor for these receptors. Together these data confirm that the NLRP3 inflammasome and caspase-1 regulate the pH of phagosomes, and thus identify a new role for caspase-1 in cellular processes.

Caspase-1 has phagosome-associated substrates that regulate pH

Phagosomes are complex intracellular compartments containing over 3000 different types of protein [26]. Caspase-1 has proteolytic activity and the observation that it accumulates on phagosomes raised the possibility that it might act locally to modify the pH and microbicidal activity by directly cleaving target proteins on the organelle. To investigate how caspase-1 might control the pH we performed a bioinformatic analysis of previously identified phagosome-associated proteins [26]. This search found over 300 proteins that had potential caspase-1 cleavage sites (Supplementary Table 1), thus identifying the candidates that might be cleaved on the phagosome after inflammasome activation to regulate the pH.

One particularly relevant set of substrates were the subunits of the NOX2 complex. In certain cells phagosomes are buffered by the phagocyte NADPH oxidase, NOX2, which generates hydroxyl groups that actively alkalinize the lumen and counteract the V-ATPase. Further analysis of the NOX2 complex identified that the potential caspase-1 cleavage sites were restricted to the cytosolic aspect of the complex and hence would be accessible to the activity of the protease (Supplementary Figure 5a). This includes Rac, which is an important, regulated component of NOX2 and indeed both Rac1 and Rac2 have previously been identified as caspase substrates [27,28]. Confirming the potential for caspase-1 to process this component of the NOX2 complex, a cleaved fragment was detected when Rac was incubated with caspase-1 (Figure 5a). As the p67-phox interaction site is at the NH_2-terminus, this processing would be predicted to disrupt the ability of Rac to interact with this component of the oxidase (Supplementary Figure 5b).

Multiple cleavage sites were also identified in p40-phox, p47-phox, p67-phox and gp91-phox, the catalytic subunit of NOX2. To further explore whether gp91-phox might be a target of caspase-1 we first performed *in silco* cleavage using the SitePrediction algorithm (Supplementary Figure 5a,b). This identified 11 potential caspase-1 cleavage sites, including a high confidence site (>99.9% probability) at D388. All of the sites in gp91-phox were cytosolic and hence potentially available to caspase-1 that was recruited to the phagosome. Many of the cleavage sites were within the COOH-terminus and would be predicted to dissociate the FAD and NADPH binding domains from the transmembrane domain, and hence disrupt the activity of the oxidase. To determine whether caspase-1 might process gp91 we first isolated membrane fractions and performed *in vitro* digestion (Figure 5b). gp91-phox is a complex protein that undergoes multiple post-translational modifications during its generation. In addition to recognizing full-length gp91-phox, which runs as a smear due to its heavy glycosylation, the anti-gp91-phox antibody (mAb 54.1) also recognizes immature forms of gp91 and fragments that have been attributed to the cleavage by intracellular proteases[29,30] thus resulting in the complex banding pattern observed by immunoblotting (Figure 5b-d and Supplementary Figure 5d-f). Nonetheless, we observed that addition of recombinant caspase-1 generated several new fragments suggesting that hydrolysis might occur at multiple sites (Figure 5b). Processing required the enzymatic activity of caspase-1, as it was blocked by the addition of YVAD (Figure 5b) and by heat inactivation of the protease (Supplementary Figure 5e).

Processing at the highest confidence caspase-1 cleavage site (D388) would be predicted to destroy the epitope recognized by mAb 54.1 that has been mapped to amino acids 383-390 31 (Supplementary Figure 5c). Therefore, to determine if processing occurred *in vivo* during infection, we took advantage of this property of 54.1 and monitored for loss of signal by immunoblot as a specific indicator of caspase-1 cleavage at D388. Consistent with endogenous processing of gp91-phox by caspase-1, infection of macrophages with *S. aureus and* Group B *Streptococcus* resulted in loss of the gp91 signal (Figure 5c). This was not due to bacterial-derived proteases from *S. aureus* as this loss was also seen in *B. subtilis* and Group B *Streptococcus* (Supplementary Figure 5f). However, this loss of signal was dependent on caspase-1, as it was not observed in caspase-1 deficient cells (Figure 5e). Taken together, these data suggest that caspase-1 might negatively regulate the NOX2 complex through hydrolysis of one or more of its subunits.

Based on our observation that caspase-1 can hydrolyse components of the NOX2 complex we hypothesized that a functional consequence of phagosome-associated caspase-1 might be to restrict NOX2 activity and ROS production in the phagosome and hence control vacuolar pH. To assess this we monitored ROS production in wild-type macrophages and macrophages deficient in inflammasome components after infection (Figure 5e-h). In wild type cells, the total cellular ROS induced by phagocytosis of *S. aureus* was also associated with a small but transient increase immediately following internalization (Figure 5e). In contrast, cells deficient in the inflammasome components all showed increased ROS activity (Figure 5e). To identify the source of this increased ROS we used a ratiometric assay and measured phagosome-associated ROS. Wild type cells showed only low levels of phagosome-associated ROS (Figure 5f-h), whereas *Nlrp3*$^{-/-}$, *Ice*$^{-/-}$ and *Asc*$^{-/-}$ cells all had greatly increased phagosome-associated ROS that persisted for 2 hours after internalization. Together these data indicate that the inflammasome can negatively regulate the levels of ROS in the lumen of the phagosome to modify the buffering capacity of the organelle, and we speculate that this is through its ability to hydrolyse components of the NOX2 complex.

The levels of ROS inversely correlated with the luminal pH when measured simultaneously in the same cells (Figure 5g) and were in keeping with caspase-1 regulating pH by modulating the buffering in the phagosome. To further evaluate this possibility, we

neutralized the oxidase by the addition of DPI and measured the pH in wild type and inflammasome deficient cells. Addition of DPI at levels that totally blocked phagosome-associated ROS production (Figure 5i), partially rescued the defect in acidification in the *Nlrp3*$^{-/-}$, *Ice*$^{-/-}$ and *Asc*$^{-/-}$ deficient cells (Figure 5i). These observations were consistent with inflammasome activation promoting acidification by decreasing buffering by the NADPH oxidase. However, despite complete inhibition of ROS, there remained a residual defect in acidification in the inflammasome deficient cells (Figure 5i) indicating that the ability of caspase-1 to modify other factors such as the V-ATPase might also be involved in how it controls the phagosome pH.

Caspase-1 regulates the pH of Gram-positive phagosomes

To establish if our model derived from studies of *S. aureus* phagosomes could be applied more broadly, we tested whether caspase-1 was involved in phagocytic processes after uptake of Gram-positive and Gram-negative bacteria. Unlike *S. aureus* early caspase-1 activation was not triggered during *E. coli* phagocytosis (Figure 2j and 6a,b). This was not due to a failure of phagocytosis as the internalization of *E. coli* into macrophages was confirmed by confocal microscopy (Supplementary Figure 1d,e). To further define which bacteria were associated with early caspase-1 activation we screened a panel of Gram-positive and Gram-negative microbes for their ability to induce FLICA staining using flow cytometry. Early caspase-1 activation was associated with internalization of all of the Gram-positive but none of the Gram-negative microbes (Figure 6c). We next tested the role of caspase-1 in regulating the activity of these different phagosomes. Phagosomes containing the Gram-positive microbes failed to acidify in macrophages that could not activate caspase-1 (Figure 6d). In contrast no defects in acidification were observed when phagosomes contained Gram-negative microbes (Figure 6e). Together these data indicate that the role of caspase-1 in phagosome acidification is cargo dependent, and that it plays an important role in controlling the intracellular fate of the Gram-positive but not Gram-negative bacteria that were tested.

Our data suggested that an important mechanism by which caspase-1 regulates the pH was by controlling the NADPH oxidase, in particular by terminating ROS generation in phagosomes. Conversely, we reasoned that phagocytosis of particles that do not induce phagosomal ROS would not require caspase-1 activation to acidify. Therefore, to establish whether the requirement for caspase-1 activation correlated with the amount of ROS generated we screened for its production during phagocytosis of our Gram-positive and Gram-negative bacteria. ROS was induced strongly after phagocytosis of *S. aureus, Bacillus subtilis* and Group B *streptococcus* (Figure 6f). In contrast *E. coli* K12, *Citrobacter rodentium* and *Enterobacter cloacae* all induced minimal ROS (Figure 6f). Taken together these data are consistent with a model in which phagosome-associated caspase-1 is required for vacuolar acidification during internalization of Gram-positive bacteria as it counteracts the buffering activity of the NOX2 complex. In contrast, phagocytosis of Gram-negative bacteria is not associated with ROS and these phagosomes can acidify independently of caspase-1 (Supplementary Figure 6).

The NLRP3 inflammasome regulates phagosome function

We next sought to determine the impact that the regulation of pH by phagosome-associated caspase-1 might have on the function of these organelles. We first validated that bacterial internalization was normal in inflammasome deficient cells using a flow cytometry based assay (Figure 7a,b). These data confirmed that equivalent levels of internalization of bacteria occurred in cells of all genotypes when infected at either low or high multiplicity of infections (MOIs). To ensure that this assay was not simply measuring binding, bacterial internalization was also confirmed both by confocal microscopy (data not shown) and EM

(Supplementary Figure 7). Acidification is essential for activation of the hydrolytic enzymes required for microbial killing. EM examination of macrophages 8 hours after infection suggested increased intra-vacuolar replication of *S. aureus* and increased escape of bacteria from the phagosome lumen into the cytosol (Figure 7c). To quantify whether these observations correlated with a failure to control the replication of bacteria in phagosomes, we performed gentamicin protection assays. These assays confirmed that the failure to activate caspase-1 not only led to a defect in phagosome acidification but also impaired the ability of macrophages to kill internalized *S. aureus* as more viable bacteria were recovered from both NLRP3 and caspase-1 deficient cells (Figure 7d). We have previously reported that the IL-6 response to *S. aureus* requires phagosome acidification[32] (Figure 7e) and hence we used production of this cytokine as another functional readout of the ability of the inflammasome to control phagosome pH. Consistent with a failure of phagosome acidification in the absence of caspase-1, treatment of macrophages with YVAD blocked production of IL-6 in response to *S. aureus* (Figure 7f). Similarly, $Ice^{-/-}$ macrophages also showed impaired IL-6 secretion (Figure 7g). As a final test of the functionality of the phagosomes we measured antigen presentation. Cross-presentation of phagocytosed antigens to CD8 T cells is thought to occur primarily from an early and non-acidified phagosome[8,15,33]. However, macrophages normally rapidly deliver antigens into acidic phagosomes and hence degrade internalized material, preventing cross-presentation. We therefore tested if inflammasome activation might antagonize the ability of phagosomes to cross-present antigens by favouring phagosome acidification. To test the cross-presentation of ovalbumin to ovalbumin-specific OT-I CD8 T cells, we measured T cell proliferation after ovalbumin was delivered to macrophages either as a soluble protein or coupled to beads that do not activate the inflammasome or coupled to *S. aureus*. WT and $Ice^{-/-}$ macrophages demonstrated equivalent ability to cross-present when ovalbumin was delivered in the absence of inflammasome activation indicating that there is no intrinsic difference in these cells (Figure 7h,i). Consistent with caspase-1 activation favouring acidification and preventing cross-presentation, WT macrophages failed to cross-present ovalbumin when delivered on *S. aureus.* In contrast, macrophages that could not activate the inflammasome (i.e. WT cells treated with YVAD and $Ice^{-/-}$ macrophages) retained the ability to cross-present ovalbumin delivered on *S. aureus* (Figure 7h,i). Thus caspase-1 activation negatively impacts cross-presentation and we speculate that this is by accelerating delivery of antigen into a degradative compartment. Taken together, these data demonstrate the profound impact that the NLRP3 inflammasome and caspase-1 can have on phagosome function and exhibit how their ability to control the pH of phagosomes impacts a number of cell-intrinsic processes important for innate and adaptive immunity.

Discussion

Much of the recent focus in innate immunity has been on the role of caspase-1 in regulating inflammatory cytokine production, with relatively little consideration for its potential to impact other innate immune processes. Nonetheless, emerging functions for caspase-1 that are independent of IL-1β and IL-18 processing, implicate this protease as a regulator of other aspects of immunity. These include unconventional protein secretion [34], activation of sterol regulatory element binding proteins [35], restriction of intracellular pathogen replication [36-38] and induction of a pro-inflammatory form of cell death termed pyroptosis [39,40]. Here we identify another function of caspase-1: to regulate phagosome pH. The pH of vacuoles controls many of the processes involved in antimicrobial defense including antigen processing and presentation [15], microbial killing [4], and TLR signalling [32,41-43]. For these reasons, the role of caspase-1 activation in regulating the pH is undoubtedly an important, but hitherto unrecognized, aspect of its role in host defense.

Our data suggest how innate immune signaling pathways can impact phagosome function by causing rapid but locally restricted post-translational modification of the proteins associated with the organelle. Specifically, the accumulation of caspase-1 on phagosomes allows its proteolytic activity to directly modify components of the organelle. However, it is unlikely that there is a single target that is sufficient to fully account for the caspase-1 phenotype. Moreover, even in the NOX2 complex, the existence of multiple sites in multiple components suggest that it would not be feasible to generate a caspase-1-resistant NOX2 complex, or recapitulate the caspase-1 deficient phenotype, using a mutagenesis approach. This targeting of multiple interacting substrates is reminiscent of findings with apoptotic caspases which have been shown in global proteomic analysis to preferentially cleave substrates that physically interact either in protein complexes or networks [44]. The dimeric nature of caspases is thought to explain the predilection of these proteases to target multiple proteins in a complex.

The ability of ROS to buffer the phagosome pH has been shown in dendritic cells where it is suggested to regulate antigen-processing [15,33]. Our studies extend these findings to demonstrate that ROS can also buffer phagosomes in macrophages and, furthermore, we show that this is relevant to certain microbial cargo and can be regulated by innate immune signals. NOX2 controls the phagosome environment as it is both the source of the ROS in the vacuole and a substrate for caspase-1. In contrast to its role in buffering pH, the role of NOX2 in activating the inflammasome is less clear. Consistent with previous reports that concluded that the source of the ROS that triggers the inflammasome is not the phagocyte oxidase, NOX2, [45] gp91-phox deficient cells retain the ability to activate caspase-1 early after phagocytosis. Instead it has been proposed that the ROS that initiates inflammasome activation is produced in a non-phagosomal compartment, such as mitochondria [46]. Our data outline an intricate relationship between the NLRP3 inflammasome and ROS, but also suggest that at least two separate sources of ROS are likely to be involved; one that acts as an initiator of inflammasome activation and another, NOX2, which is a local substrate of caspase-1 on the phagosome that modifies the pH. We propose that the requirement for caspase-1 in acidification segregates with ROS production during phagocytosis, not because ROS is required to activate the inflammasome, but rather because NOX2 buffers the pH of certain phagosomes and in these cases must be targeted by caspase-1 for acidification to proceed.

Consistent with our work identifying a role for caspase-1 in regulating the pH of phagosomes containing Gram-positive microbes, it is notable that previous work has implicated the inflammasome in restricting replication of *Mycobacterium tuberculosis* [36]. In contrast, phagosomes containing Gram-negative bacteria do not demonstrate the same dependence on caspase-1 for phagosome acidification, indicating that the ability of caspase-1 to regulate phagosome pH is cargo dependent. We propose that the paucity of ROS after Gram-negative phagocytosis obviates the need for caspase-1, as it is not required to inactivate the oxidase in the vacuole for acidification to occur. This simple difference explains why Gram-positive phagosomes must be accompanied by caspase-1 activation for complete acidification to occur whereas Gram-negative phagosomes can acidify independently of caspase-1. Nonetheless, maturation of Gram-negative phagosomes is a regulated process and, as an example, caspase-11 regulates maturation of *Legionella* vacuoles through a mechanism distinct from that described herein [37,38,47]. It is evident therefore that there are multiple mechanisms that control different aspects of phagosome maturation, and that the relative importance of each is determined in part by the nature of the microbial cargo.

Whether caspase-1 similarly regulates the intracellular fate of non-microbial NLRP3 agonists remains to be determined, but the potential is enticing and would provide new

perspectives on the role of the NLRP3-inflammasome in sterile inflammation. Finally, these data raise the intriguing possibility that pathogens that block caspase activation [48] may do so not simply to regulate the production of inflammatory cytokines but also to evade cellular immunity by specifically perturbing the function of phagosomes, compartments that otherwise restrict the intracellular replication of microbes and are crucial in initiating both innate and adaptive immune responses.

METHODS

Mice and Cell Culture

C57BL/6J, B6.129S6-*Cybb*^{tm1Din}/J, 129X1/SvJ and 129P3/J mice were from Jackson Laboratory (Bar Harbor, ME). *Myd88*$^{-/-}$ mice were from M. Freeman (MGH, MA), OT-I transgenic mice (B6.129S6-*Rag2*^{tm1Fwa}Tg(TcraTcrb)1100Mjb) were from J.R. Mora (MGH, MA) and *Tlr2*$^{-/-}$ mice were from R. Medzhitov (Yale University School of Medicine, CT). Mice were handled under a protocol approved by the Subcommittee on Research Animal Care at MGH.

Thioglycollate-elicited peritoneal macrophages and Bone Marrow-derived (BM) macrophages were grown as described [32,49]. Immortalized WT, *Ice*$^{-/-}$, *Asc*$^{-/-}$, *Nlrp3*$^{-/-}$ and *MyD88/TRIF*$^{-/-}$ BM macrophage cell lines were cultured as described [50-52]. HEK293T, J774.1 and RAW 264.7 cell lines (ATCC) were maintained according to ATCC's recommendations.

Typically macrophages were pre-chilled for 15 min on ice in media with 1% FBS before adding bacteria. Bacterial clusters were disrupted by repeated passage through a 30-gauge needle. Cells with bacteria were kept on ice for 30-40 min allowing the synchronization of phagocytosis. Macrophages were then incubated at 37°C for the indicated times.

Bacteria

S. aureus Reynolds strain capsular serotype 5 (Cp5) (JC Lee, Brigham and Women's Hospital, MA), *S. aureus* Newman strain and isogenic mutants (ΔAgr, ΔSar, Δ Agr/Sar) (F. Ausubel, MGH, MA), and Group B *Streptococci* (strain GBS type III COH-1; M. Wessels, Boston Children's Hospital, MA) were grown as described [32]. *B. subtilis, C. rodentum, E. cloacae* (K. Fitzgerald, University of Massachusetts, MA) and *E. coli* (strain K12; ATCC) were grown at 37°C in LB medium overnight. When noted bacteria were heat-inactivated (HI) at 65°C for 30 min. Bacteria labelling was as described [49,53].

Phagocytosis and phagosome acidification assays were performed as described [49]. In some cases, before adding bacteria, macrophages were pretreated for 1h with Bafilomycin A (Sigma-Aldrich, 100 nM) or Cytochalasin D (Sigma-Aldrich, 10 μM) or for 2h with YVAD or ZVAD inhibitors (Calbiochem). Where noted BM macrophages were pretreated with Ultrapure LPS (*E. coli* 0111:B4, Invivogen, 100 ng/ml) for 3 h and ATP (Sigma-Aldrich, 5 mM) for 15 min before placing cells on ice. ATP was washed from the cells together with bacteria after incubation for 5 min in a 37°C water bath.

Phagosome dissipation assays were modified from previously described protocols [9,23]. Macrophages were treated as above and indicated inhibitors were added after 30 min of phagosome acidification. Equivalent amounts of DMSO were used as a vehicle control. Cells were collected, washed and analyzed as described above 1, 5, 15 and 60 min after adding the inhibitors.

Total ROS production

Macrophages were loaded with H2DCFDA (Invitrogen, 10 μM) in medium with 1% FBS for 40 min at 37°C. Cells were chilled for 15 min on ice and bacteria were added (MOI 50). Cells were centrifuged at 515 × g for 4 min and incubated at 37°C for the indicated period of time. Cells were washed, detached and immediately analyzed by flow cytometry to determine MFI of H2DCFDA. Where noted, the ROS inhibitor Diphenyleneiodonium chloride (DPI, Sigma-Aldrich, 2 or 5μM) was added to the wells 10 min before incubation on ice.

Measurement of ROS production in the phagosome was adapted [53] and where noted macrophages were pretreated for 1h with Bafilomycin A (100 nM) and 10 min with DPI (5mM).

Caspase-1 activation by FACS and Western Blot

For FACS-based monitoring of caspase-1 activation live or HI *S. aureus* Reynolds $CP5^+$ (MOI 50) or latex beads (Polysciences, 20 beads per cell) were added to cells, and following synchronization were incubated at 37°C for the indicated periods of time. Cells were washed and media was replaced with Fluorochrome-Labeled Inhibitors of Caspase-1 (FLICA, FAM-YVAD-FMK) reagent (Immunochemistry) and incubated for 1h. Caspase-1 should be active first before labeling with FLICA as addition of FLICA inhibits all subsequent caspase-1 activation. Next, cells were washed and analyzed live by FACS. In some experiments cells were pretreated with Bafilomycin A (100 nM) or Cytochalasin D (10 μM) for 1h; DPI (2 μM) for 10 min; or Bay11-7085 (Sigma-Aldrich, 20 μM) or NF-κB Activation Inhibitor 6-Amino-4-(4-phenoxyphenylethylamino) quinazoline (QNZ, Calbiochem, 100nM) for 30 min before placing cells on ice. Inhibitors were washed from the cells together with bacteria before adding FLICA.

To monitor caspase-1 activation by Western blot, BM macrophages were infected with *S. aureus* as indicated. Processing of caspase-1 was analyzed by immunoblotting of cell lysates or supernatants using anti-caspase-1 P10 (M-20, Santa Cruz Biotechnology). Some western blot images were cut and rearranged to remove irrelevant information; however, all lanes are from the same blot with the same exposure and contrast.

Confocal imaging

For imaging of active caspase-1, BM macrophages were stimulated with live *S. aureus* or *E. coli* (MOI 10) or with beads (10 or 20 beads per cell) for 30 min or 1h. Media was then replaced with FAM-YVAD-FMK or SR-VAD-FMK and incubated for 1h. Cells were washed and imaged live. Some cells were fixed in 4% PFA and cell membrane was stained with Alexa Fluor 647-conjugated cholera toxin subunit B (ChTxB, Invitrogen). Cell nuclei and bacterial DNA were stained with Hoescht 33342. Cells were imaged immediately as FLICA staining is not stable after fixation and does not tolerate permeabilization. In some experiments cells were pretreated with Cytochalasin D (10 μM) for 1h; LPS (100 ng/ml) for 3h and ATP (5 mM) for 15 min before FLICA addition.

RAW 264.7, transfected by Amaxa electroporation with RFP-caspase-1 (C285A) (C. Stehlik, Northwestern University, IL) or BM macrophages were incubated with live *S. aureus* Reynolds $CP5^+$ (MOI 10) or latex beads (10 beads per cell) at 37°C for 30 min or 1h following synchronization. For caspase-1 staining by antibody, BM macrophages were fixed with 4% PFA, permeabilized, blocked and incubated overnight at 4°C in caspase-1 p10 antibody (M-20, 1:50). Cells were washed and incubated in secondary Alexa 546 goat anti-rabbit antibody (1:250) for 1h at RT. Cells were washed, cell nuclei and bacteria DNA were stained with Hoechst 33342.

Cells were imaged using 40× objective (aperture 0.6) and 100× oil objective (aperture 1.4) and Nikon Ti (Eclipse) inverted microscope with Ultraview Spinning Disc (CSU-X1) confocal scanner (Perkin Elmer). Images were captured with an Orca-ER Camera using Volocity (Perkin Elmer). Post-acquisition analysis was performed using Volocity software.

Electron Microscopy

Macrophages following synchronization on ice were loaded with live *S. aureus* (MOI 10) at 37°C for 1h. Cells were washed twice in PBS and further incubated for 7h. Electron microscopy was performed by The Microscopy Core of the Program in Membrane Biology at MGH using a JEOL 1011 transmission electron microscope at 80 kV with an AMT digital imaging system (Advanced Microscopy Techniques, MA).

***S. aureus* survival in macrophages** were performed as described [49].

Cytokine production in cell-culture supernatants was assayed using DuoSet ELISA (R&D Systems).

Antigen cross-presentation

BM macrophages or WT or *Ice*$^{-/-}$ macrophage cell lines were incubated with soluble ovalbumin (OVA) (0.5 mg/ml), 3μm OVA-coated latex beads (10 beads per cell) or OVA-coated HI *S. aureus* (MOI 10) for 1h for antigen loading. In some experiments cells were pretreated for 1h with YVAD inhibitor (100 mM). After 1h antigen and inhibitor were washed, and macrophages were further co-cultured with CFSE-labeled OT-1 CD8^{+} T cells for 3 days at a ratio of 1:4 (BMDM: T cells). Next, cells were labeled with CD8 antibody and decrease of CFSE staining on CD8^{+} T cells was measured by FACS. CD8^{+} T cells were isolated from spleens of OT-I transgenic mice using magnetic beads (Miltenyi Boitec, CA) according to manufacturer's protocol and stained with 5 mM CFSE for 10 min at RT. For preparation of particulate antigen, OVA was conjugated to latex beads or HI *S. aureus* by passive adsorption as described [54].

Rac and GP91-phox cleavage assays, in vivo processing and immunoblotting

HEK 293T cells were transfected with HA-Rac1 (E. Lemichez C3M INSERM U1065) with Fugene (Roche) and lysates were used as substrates in a cleavage assay with recombinant mouse caspase-1 (Biovision) as previously described [55]. Samples were separated by SDS/PAGE and followed by immunoblot analysis for anti-HA (16B12, Covance).

To test gp91-phox cleavage, cell membranes were isolated from BM macrophages and were assayed as above using anti-gp91phox (54.1, Santa Cruz Biotechnology). In some experiments recombinant caspase-1 was heat inactivated for 10 min at 95°C.

To test gp91-phox processing by caspase-1 in vivo, BM macrophages or WT or *Ice*$^{-/-}$ macrophage cell lines were infected as indicated (MOI 50). Bacteria were added to cells, centrifuged 515×g for 4 min and incubated at 37°C for indicated period of time. Cells were washed and cell membranes were isolated. Samples were separated by SDS/PAGE and immunoblotted with anti-gp91phox (54.1). Some western blot images were cut and rearranged to remove irrelevant information; however, all lanes are from the same blot with the same exposure and contrast.

Statistics

All data are typically presented as a pool of three experiments (mean ± s.e.m), or as a single experiment representative of three or more independent experiments (mean ± s.d). Treatment groups were compared using the paired Student's t test.

Supplementary Material

Refer to Web version on PubMed Central for supplementary material.

Acknowledgments

This work was funded by grants from the NIH/NIAID to LMS (RO1 AI079198) and KAF (RO1 AI093752), NIH/NIA to KJM (RO1 AG020255) grants from the Crohns' and Colitis and Hood foundations and NIH/NIDDK to ALH (RO1 DK093695) and postdoctoral fellowships from MGH ECOR to AS and NERCE/BEID (U54 AI057159) to NP. Electron microscopy was performed by M. McKee in the Microscopy Core of the Center for Systems Biology.

References

1. Greenberg S, Grinstein S. Phagocytosis and innate immunity. Curr Opin Immunol. 2002; 14:136–145. [PubMed: 11790544]
2. Vieira OV, Botelho RJ, Grinstein S. Phagosome maturation: aging gracefully. Biochem J. 2002; 366:689–704. [PubMed: 12061891]
3. Desjardins M, Huber LA, Parton RG, Griffiths G. Biogenesis of phagolysosomes proceeds through a sequential series of interactions with the endocytic apparatus. J Cell Biol. 1994; 124:677–688. [PubMed: 8120091]
4. Scott CC, Botelho RJ, Grinstein S. Phagosome maturation: a few bugs in the system. J Membr Biol. 2003; 193:137–152. [PubMed: 12962275]
5. Stuart LM, Ezekowitz RA. Phagocytosis: elegant complexity. Immunity. 2005; 22:539–550. [PubMed: 15894272]
6. Meresse S, et al. Controlling the maturation of pathogen-containing vacuoles: a matter of life and death. Nat Cell Biol. 1999; 1:E183–188. [PubMed: 10560000]
7. Wolf AJ, et al. Phagosomal degradation increases TLR access to bacterial ligands and enhances macrophage sensitivity to bacteria. J Immunol. 2011; 187:6002–6010. [PubMed: 22031762]
8. Amigorena S, Savina A. Intracellular mechanisms of antigen cross presentation in dendritic cells. Curr Opin Immunol. 2010; 22:109–117. [PubMed: 20171863]
9. Lukacs GL, Rotstein OD, Grinstein S. Phagosomal acidification is mediated by a vacuolar-type H(+)-ATPase in murine macrophages. J Biol Chem. 1990; 265:21099–21107. [PubMed: 2147429]
10. Yates RM, Hermetter A, Russell DG. The kinetics of phagosome maturation as a function of phagosome/lysosome fusion and acquisition of hydrolytic activity. Traffic. 2005; 6:413–420. [PubMed: 15813751]
11. Forgac M. Vacuolar ATPases: rotary proton pumps in physiology and pathophysiology. Nat Rev Mol Cell Biol. 2007; 8:917–929. [PubMed: 17912264]
12. Sun-Wada GH, Tabata H, Kawamura N, Aoyama M, Wada Y. Direct recruitment of H+-ATPase from lysosomes for phagosomal acidification. J Cell Sci. 2009; 122:2504–2513. [PubMed: 19549681]
13. Brisseau GF, et al. Interleukin-1 increases vacuolar-type H+-ATPase activity in murine peritoneal macrophages. J Biol Chem. 1996; 271:2005–2011. [PubMed: 8567651]
14. Trombetta ES, Ebersold M, Garrett W, Pypaert M, Mellman I. Activation of lysosomal function during dendritic cell maturation. Science. 2003; 299:1400–1403. [PubMed: 12610307]
15. Savina A, et al. NOX2 controls phagosomal pH to regulate antigen processing during crosspresentation by dendritic cells. Cell. 2006; 126:205–218. [PubMed: 16839887]
16. Underhill DM, et al. The Toll-like receptor 2 is recruited to macrophage phagosomes and discriminates between pathogens. Nature. 1999; 401:811–815. [PubMed: 10548109]
17. Ozinsky A, et al. The repertoire for pattern recognition of pathogens by the innate immune system is defined by cooperation between toll-like receptors. Proc Natl Acad Sci U S A. 2000; 97:13766–13771. [PubMed: 11095740]
18. Underhill DM, Gantner B. Integration of Toll-like receptor and phagocytic signaling for tailored immunity. Microbes Infect. 2004; 6:1368–1373. [PubMed: 15596122]

19. Blander JM, Medzhitov R. Regulation of phagosome maturation by signals from toll-like receptors. Science. 2004; 304:1014–1018. [PubMed: 15143282]
20. Yates RM, Russell DG. Phagosome maturation proceeds independently of stimulation of toll-like receptors 2 and 4. Immunity. 2005; 23:409–417. [PubMed: 16226506]
21. Shimada T, et al. Staphylococcus aureus evades lysozyme-based peptidoglycan digestion that links phagocytosis, inflammasome activation, and IL-1beta secretion. Cell Host Microbe. 2010; 7:38–49. [PubMed: 20114027]
22. Grabarek J, Darzynkiewicz Z. In situ activation of caspases and serine proteases during apoptosis detected by affinity labeling their enzyme active centers with fluorochrome-tagged inhibitors. Exp Hematol. 2002; 30:982–989. [PubMed: 12225789]
23. Hackam DJ, et al. Regulation of phagosomal acidification. Differential targeting of Na+/H+ exchangers, Na+/K+-ATPases, and vacuolar-type H+-atpases. J Biol Chem. 1997; 272:29810–29820. [PubMed: 9368053]
24. Lukacs GL, Rotstein OD, Grinstein S. Determinants of the phagosomal pH in macrophages. In situ assessment of vacuolar H(+)-ATPase activity, counterion conductance, and H+ “leak”. J Biol Chem. 1991; 266:24540–24548. [PubMed: 1837024]
25. Steinberg BE, Huynh KK, Grinstein S. Phagosomal acidification: measurement, manipulation and functional consequences. Biochem Soc Trans. 2007; 35:1083–1087. [PubMed: 17956285]
26. Trost M, et al. The phagosomal proteome in interferon-gamma-activated macrophages. Immunity. 2009; 30:143–154. [PubMed: 19144319]
27. Zhang B, Zhang Y, Shacter E. Caspase 3-mediated inactivation of rac GTPases promotes drug-induced apoptosis in human lymphoma cells. Mol Cell Biol. 2003; 23:5716–5725. [PubMed: 12897143]
28. Shao W, Yeretssian G, Doiron K, Hussain SN, Saleh M. The caspase-1 digestome identifies the glycolysis pathway as a target during infection and septic shock. J Biol Chem. 2007; 282:36321–36329. [PubMed: 17959595]
29. Baniulis D, et al. Evaluation of two anti-gp91phox antibodies as immunoprobes for Nox family proteins: mAb 54.1 recognizes recombinant full-length Nox2, Nox3 and the C-terminal domains of Nox1-4 and cross-reacts with GRP 58. Biochim Biophys Acta. 2005; 1752:186–196. [PubMed: 16140048]
30. Foubert TR, et al. Identification of a spectrally stable proteolytic fragment of human neutrophil flavocytochrome b composed of the NH2-terminal regions of gp91(phox) and p22(phox). J Biol Chem. 2001; 276:38852–38861. [PubMed: 11504718]
31. Burritt JB, Quinn MT, Jutila MA, Bond CW, Jesaitis AJ. Topological mapping of neutrophil cytochrome b epitopes with phage-display libraries. J Biol Chem. 1995; 270:16974–16980. [PubMed: 7622517]
32. Ip WK, et al. Phagocytosis and phagosome acidification are required for pathogen processing and MyD88-dependent responses to Staphylococcus aureus. J Immunol. 184:7071–7081. [PubMed: 20483752]
33. Mantegazza AR, et al. NADPH oxidase controls phagosomal pH and antigen cross-presentation in human dendritic cells. Blood. 2008; 112:4712–4722. [PubMed: 18682599]
34. Keller M, Ruegg A, Werner S, Beer HD. Active caspase-1 is a regulator of unconventional protein secretion. Cell. 2008; 132:818–831. [PubMed: 18329368]
35. Gurcel L, Abrami L, Girardin S, Tschopp J, van der Goot FG. Caspase-1 activation of lipid metabolic pathways in response to bacterial pore-forming toxins promotes cell survival. Cell. 2006; 126:1135–1145. [PubMed: 16990137]
36. Master SS, et al. Mycobacterium tuberculosis prevents inflammasome activation. Cell Host Microbe. 2008; 3:224–232. [PubMed: 18407066]
37. Akhter A, et al. Caspase-7 activation by the Nlrc4/Ipaf inflammasome restricts Legionella pneumophila infection. PLoS Pathog. 2009; 5:e1000361. [PubMed: 19343209]
38. Amer A, et al. Regulation of Legionella phagosome maturation and infection through flagellin and host Ipaf. J Biol Chem. 2006; 281:35217–35223. [PubMed: 16984919]

39. Fernandes-Alnemri T, et al. The pyroptosome: a supramolecular assembly of ASC dimers mediating inflammatory cell death via caspase-1 activation. Cell Death Differ. 2007; 14:1590–1604. [PubMed: 17599095]
40. Lamkanfi M, Dixit VM. The inflammasomes. PLoS Pathog. 2009; 5:e1000510. [PubMed: 20041168]
41. Herskovits AA, Auerbuch V, Portnoy DA. Bacterial ligands generated in a phagosome are targets of the cytosolic innate immune system. PLoS Pathog. 2007; 3:e51. [PubMed: 17397264]
42. Park B, et al. Proteolytic cleavage in an endolysosomal compartment is required for activation of Toll-like receptor 9. Nat Immunol. 2008; 9:1407–1414. [PubMed: 18931679]
43. Ewald SE, et al. The ectodomain of Toll-like receptor 9 is cleaved to generate a functional receptor. Nature. 2008; 456:658–662. [PubMed: 18820679]
44. Mahrus S, et al. Global sequencing of proteolytic cleavage sites in apoptosis by specific labeling of protein N termini. Cell. 2008; 134:866–876. [PubMed: 18722006]
45. Meissner F, et al. Inflammasome activation in NADPH oxidase defective mononuclear phagocytes from patients with chronic granulomatous disease. Blood. 2010; 116:1570–1573. [PubMed: 20495074]
46. Zhou R, Yazdi AS, Menu P, Tschopp J. A role for mitochondria in NLRP3 inflammasome activation. Nature. 2011; 469:221–225. [PubMed: 21124315]
47. Akhter A, et al. Caspase-11 promotes the fusion of phagosomes harboring pathogenic bacteria with lysosomes by modulating actin polymerization. Immunity. 2012; 37:35–47. [PubMed: 22658523]
48. Taxman DJ, Huang MT, Ting JP. Inflammasome inhibition as a pathogenic stealth mechanism. Cell Host Microbe. 2010; 8:7–11. [PubMed: 20638636]
49. Sokolovska A, Becker CE, Stuart LM. Measurement of phagocytosis, phagosome acidification, and intracellular killing of Staphylococcus aureus. Curr Protoc Immunol. 2012:30. Chapter 14, Unit14. [PubMed: 23129153]
50. Halle A, et al. The NALP3 inflammasome is involved in the innate immune response to amyloid-beta. Nat Immunol. 2008; 9:857–865. [PubMed: 18604209]
51. Hornung V, et al. Silica crystals and aluminum salts activate the NALP3 inflammasome through phagosomal destabilization. Nat Immunol. 2008; 9:847–856. [PubMed: 18604214]
52. Kasperkovitz PV, Cardenas ML, Vyas JM. TLR9 is actively recruited to Aspergillus fumigatus phagosomes and requires the N-terminal proteolytic cleavage domain for proper intracellular trafficking. J Immunol. 2010; 185:7614–7622. [PubMed: 21059889]
53. Savina A, Vargas P, Guermonprez P, Lennon AM, Amigorena S. Measuring pH, ROS production, maturation, and degradation in dendritic cell phagosomes using cytofluorometry-based assays. Methods Mol Biol. 2010; 595:383–402. [PubMed: 19941126]
54. Ramachandra L, Boom WH, Harding CV. Class II MHC antigen processing in phagosomes. Methods Mol Biol. 2008; 445:353–377. [PubMed: 18425462]
55. Miggin SM, et al. NF-kappaB activation by the Toll-IL-1 receptor domain protein MyD88 adapter-like is regulated by caspase-1. Proc Natl Acad Sci U S A. 2007; 104:3372–3377. [PubMed: 17360653]

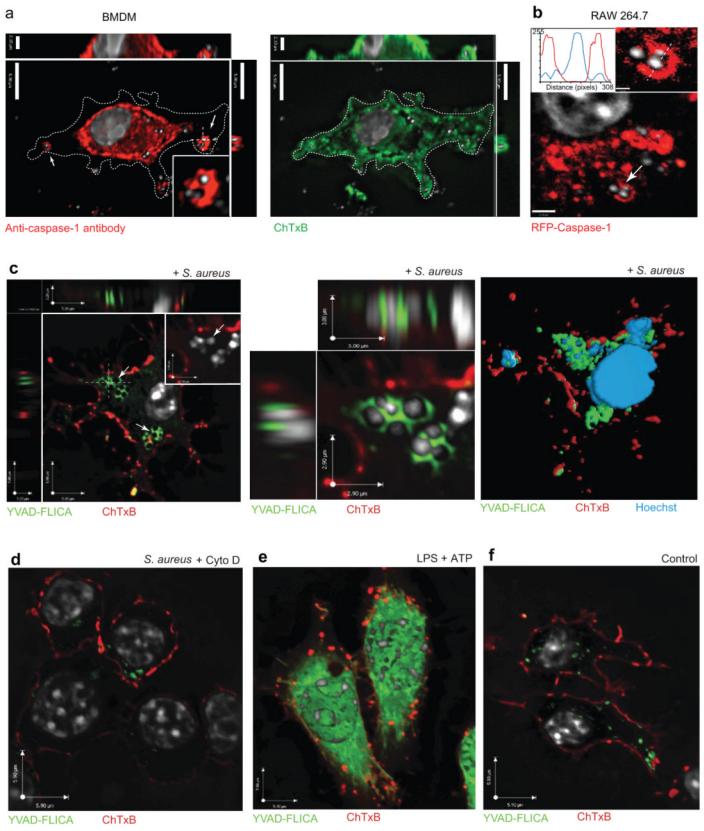

Figure 1. Active caspase-1 is recruited to *S. aureus* phagosomes

a-b, The localization of total caspase-1 was determined 30 minutes after infection with *S. aureus* (MOI: 10) in **a,** Bone-marrow derived macrophages (BMDM) stained with anti-caspase-1 antibody (left) and cholera toxin (right) or **b,** RAW 264.7 macrophages transfected with RFP-caspase-1. Caspase-1, red; Cell and bacterial DNA, white. **c-f**, Localization of active caspase-1 in BMDMs was determined by staining with FLICA. **c, left panel**, Live *S. aureus* (MOI: 10); **middle panel**, high magnification of phagosome-associated active caspase-1 (YVAD-FLICA) staining and **right panel**, three-dimensional rendering model of phagosome-associated active caspase-1. **d**, *S. aureus* (MOI: 10) with Cytochalasin D (10 μM), **e**, Localization of active caspase-1 in response to LPS and ATP, and **f,** control untreated cells. Cell nuclei and bacterial DNA were labeled with Hoechst (white); plasma membrane was stained with Alexa-647-conjugated cholera toxin B (red); and active caspase-1 with YVAD-FLICA reagent (green). Caspase-1 activation was measured 1h post-infection by staining with FLICA for 1h. Data are representative of three independent experiments.

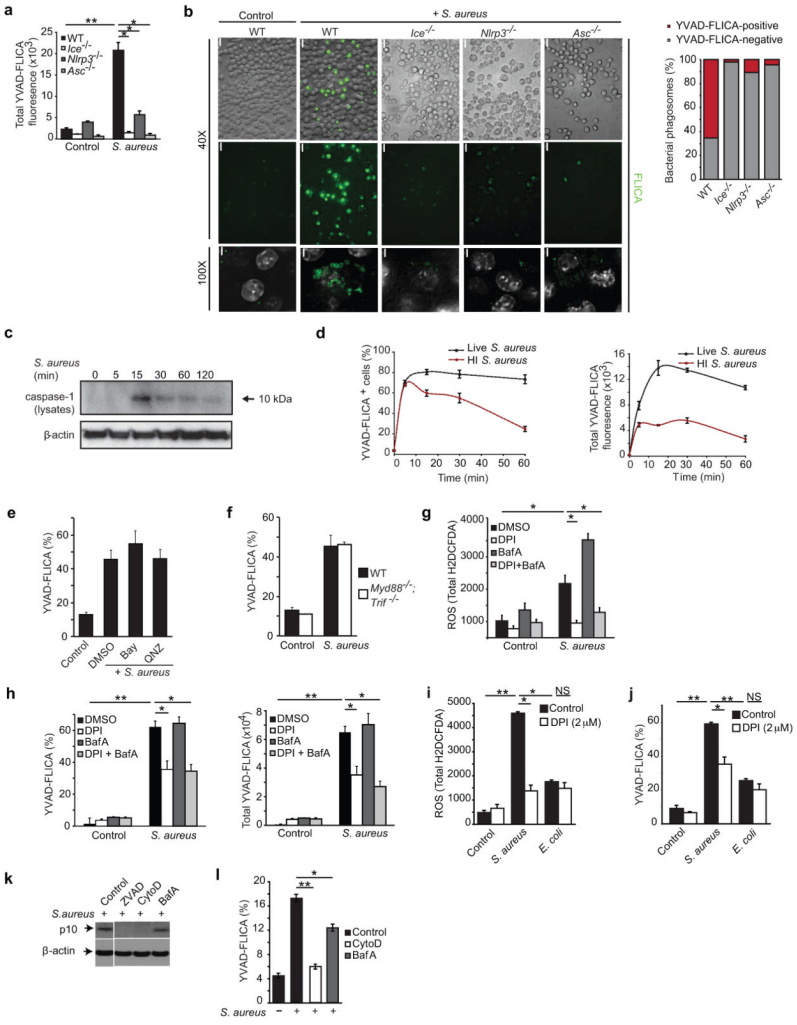

Figure 2. Phagocytosis of *S. aureus* triggers early activation of the NLRP3 inflammasome and caspase-1

a, Active caspase-1 was determined by staining with FLICA 15 min after *S. aureus* internalization and measured by flow cytometry (live *S. aureus* MOI: 50) or **b, left panels,** microscopy (live *S. aureus* MOI: 10) in WT BMDM cell lines and cells deficient in inflammasome components; Green, active caspase-1 as measured by YVAD-FLICA. White, nuclei and bacterial DNA. Scale bars in 40× panels represents 5.9μm and 100× panel 2.9μm. **Right**, quantification of the number of caspase-1 positive phagosomes calculated as a percentage of total phagosomes in each cell type WT - 237 phagosomes, *Ice*$^{-/-}$ - 185 phagosomes, *Nlrp3*$^{-/-}$ - 157 phagosomes, *Asc*$^{-/-}$ −183 phagosomes. **c**, Kinetics of caspase-1 activation in response to live *S. aureus* (MOI: 100) was determined in BMDM by immunoblot of Caspase-1 p10 in total cell lysates. **d**, Kinetics of caspase-1 activation in response to *S. aureus* in BMDM was measured by flow cytometry after internalization of live (black) and heat-inactivated (HI) (red) *S. aureus* (MOI: 50). The amount of caspase-1 activation was measured by the addition of YVAD-FLICA, which acts to both inhibit further activation and label the protease that is active at the time of addition (Supplementary Figure 2e,f). The time indicates when FLICA was added to the cells after *S. aureus* uptake and then incubated for a further 1 hour. Left panel % FLICA positive cells, right panel, total YVAD-FLICA fluorescence. **e-f,** YVAD-FLICA activation in the presence of **e,** the NF-kB

inhibitors BAY 11-7085 (20 μM) and QNZ (100 nM) and **f**, in *Myd88*$^{-/-}$ *Trif*$^{-/-}$ cells. **g,** Total cellular ROS production in control and live *S. aureus* (MOI: 50) infected BMDM treated with Bafilomycin A (100 nM) and/or DPI (2μM). **h,** Early caspase-1 activation by live *S. aureus* (MOI: 50) was measured by flow cytometry of YVAD-FLICA in BMDM treated with Bafilomycin A (100 nM) and/or DPI (2μM). **i**, Total cellular ROS and **j,** YVAD-FLICA activity induced by live *S. aureus* or *E. coli* (bacterial MOI: 50) uptake in control BMDM or macrophages treated with DPI (2 μM). In **g-j**, Bafilomycin A was added 30 min and DPI was added 10 min prior to infection. ROS was measured at 15 minutes; and FLICA was added at 15 min post-internalization for 1h. **k**, Peritoneal macrophages were infected for 2h with live *S. aureus* (MOI: 25) in the presence or absence of the pan-caspase inhibitor ZVAD (100 μM), Cytochalasin D (10 μM) and V-ATPase inhibitor Bafilomycin A (100 nM). Late caspase-1 activation was determined by immunoblotting for caspase-1 p10 in the culture supernatants. **l,** Peritoneal macrophages were infected for 1h with live *S. aureus* (MOI: 25) with or without Cytochalasin D (10 μM) or Bafilomycin A (100 nM) and stained with FLICA for 1h. Late caspase activity was measured by FACS analysis of FLICA labeled cells. Data are representative of three or more independent experiments (mean ± s.d). * $p<0.01$, ** $p<0.001$ by Student's t-test.

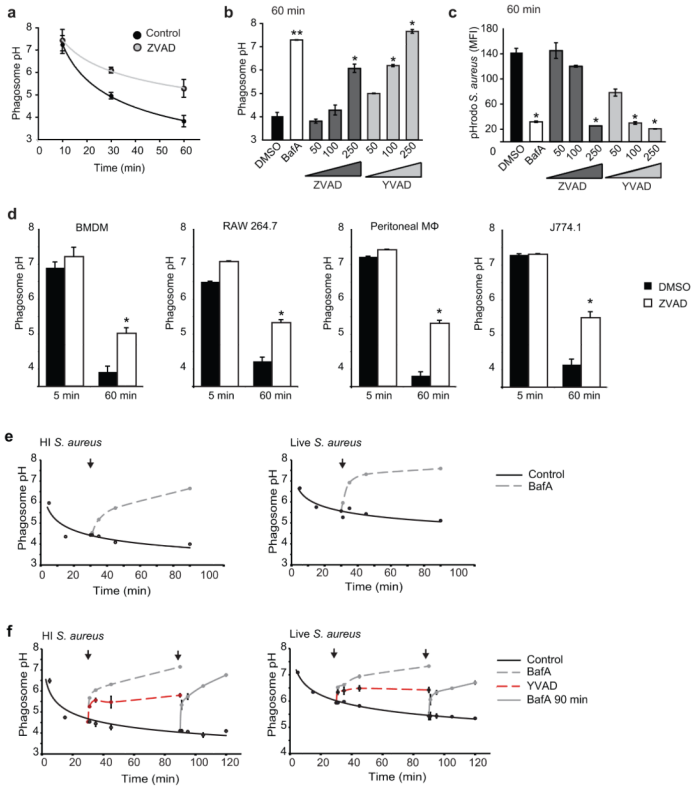

Figure 3. Caspase-1 inhibition blocks the acidification of *S. aureus*-containing phagosomes

a, Kinetics of HI *S. aureus* phagosome acidification in peritoneal macrophages pre-treated for 2h with ZVAD (100 μM). **b-c,** Phagosome pH in peritoneal macrophages was measured 1h after uptake of HI *S. aureus* with or without pre-treatment with pan-caspase inhibitor ZVAD (μM; dark grey), caspase-1 inhibitor YVAD (μM; light grey) and Bafilomycin A (100 nM; white bar). The pH was measured by a ratiometric assay (**b**) and using FACS analysis of pHrodo bacteria (**c**). Data in **a-c** are from one experiment representative of three (mean ± s.d.). **d,** The pH of the phagosomes containing HI *S. aureus* was measured in the absence (black bars) and presence (white bars) of the pan-caspase inhibitor, ZVAD (200 μM) in BMDM, RAW 264.7 macrophages, peritoneal macrophages and J774.1 cells. * $p<0.01$, ** $p<0.001$ by Student's t-test. **e,** pH of phagosomes containing HI (left panel) or live (right panel) *S. aureus* was monitored in BMDM after the addition of Bafilomycin A (400nM) or control vehicle (DMSO) at 30 minutes. **f,** pH of phagosomes containing HI (left panel) and live (right panel) *S. aureus* was monitored in BMDM after addition of YVAD (250μM) or control vehicle (DMSO) at 30 minutes. The pH of phagosomes after addition of Bafilomycin A (400nM) at 30 and 90 minutes are shown as a positive control. Arrows indicate the time of addition of the drugs. Data are representative of three independent experiments (mean ± s.d).

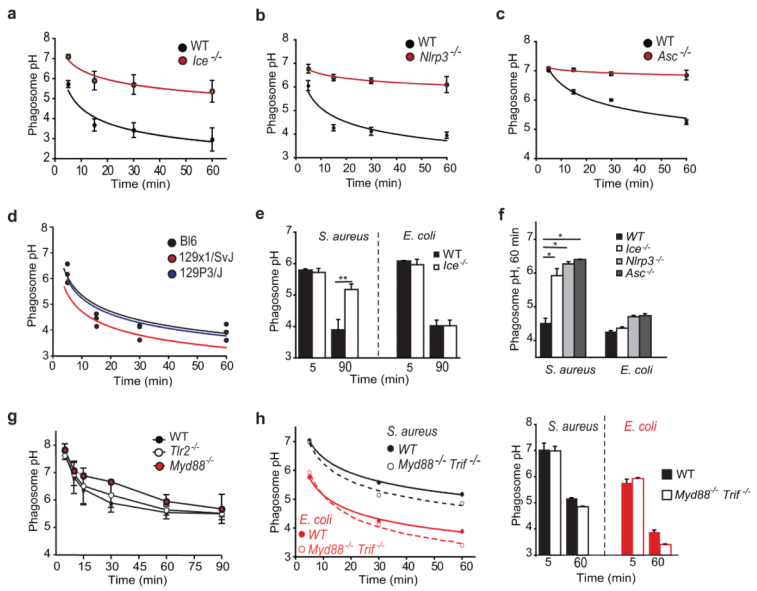

Figure 4. The NLRP3 inflammasome regulates acidification of *S. aureus* phagosomes

a-d, The kinetics of acidification of HI *S. aureus* phagosomes in WT and *Ice*$^{-/-}$ (**a**), *Nlrp3*$^{-/-}$ (**b**), *Asc*$^{-/-}$ (**c**) BMDM cell lines and 129P3/J and 129x1/SvJ (**d**) BMDM. Data from a pool of three independent experiments (mean ± s.e.m). (WT, black lines; knockouts, red lines). **e-f**, Acidification of HI *S. aureus* and *E. coli* phagosomes in WT, *Ice*$^{-/-}$, *Nlrp3*$^{-/-}$ and *Asc*$^{-/-}$ BMDM cell lines. **g,** Kinetics of acidification of HI *S. aureus* phagosomes in *Myd88*$^{-/-}$ and *Tlr2*$^{-/-}$ BM macrophages. **h**, Kinetics of acidification of HI *S. aureus* and *E. coli* phagosomes in WT and *Myd88*$^{-/-}$ *Trif*$^{-/-}$ BM macrophage cell lines. Phagosome pH 5 and 60 mins after internalization of *S. aureus* or *E. coli* in WT and *Myd88*$^{-/-}$ *Trif*$^{-/-}$ BM macrophage cell lines . (**a-c)** Data are presented as a pool of three or more experiments (mean ± s.e.m), **(d-h)** Data are representative of three or more independent experiments. * p<0.01, **p<0.001 by Student's t-test.

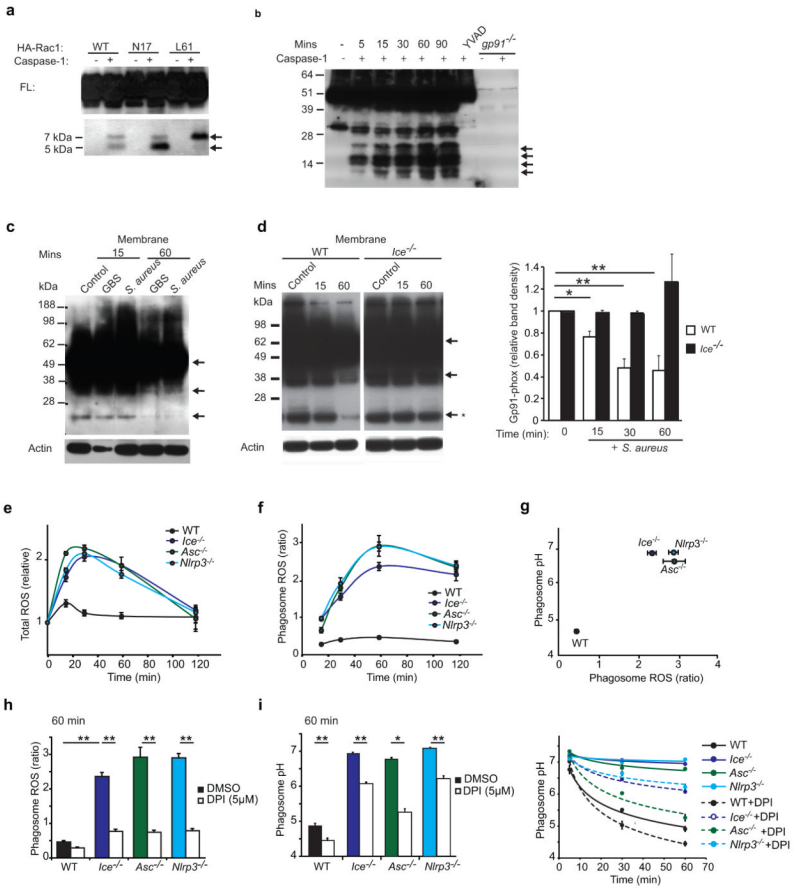

Figure 5. Caspase-1 has phagosome-associated substrates that regulate pH

a, Lysates from HEK293T cells expressing HA-Rac1WT, N17 and L61 mutants were treated with recombinant caspase-1 and immunoblotted for HA. **b**, Membrane preparations from BMDM were treated with recombinant caspase-1 and immunoblotted for gp91-phox. Arrows in **a** and **b**, indicate the cleaved fragments of Rac and gp91-phox. **c-d** BMDM were infected with *S. aureus* or Group B *Streptococcus* (MOI: 50) **(c)** and WT and *Ice*$^{-/-}$ macrophage cell lines were infected with *S. aureus* (MOI: 50) **(d, left panel)** for the stated times and membranes isolated and immunoblotted for gp91-phox. Arrows indicate loss of gp91-phox signal due to epitope disruption. **d, right panel,** time course quantifying the intensity of the 22-25 kDa band (marked with and asterisk in **left panel**) in WT (white bars) and *Ice*$^{-/-}$ (black bars) cells. Data from a pool of three independent experiments (mean ± s.e.m). **e,** Total ROS and **f,** Phagosome-associated ROS was measured in WT, *Ice*$^{-/-}$, Asc$^{-/-}$ and *Nlrp3*$^{-/-}$ BM macrophage cell lines after HI *S. aureus* (MOI: 10) phagocytosis. **g**, Correlation of phagosome pH and ROS measured in the same cells. **h**, Phagosome ROS and **i,** pH was measured in the presence and absence of DPI in WT, *Ice*$^{-/-}$, Asc$^{-/-}$ *and Nlrp3*$^{-/-}$ BM macrophage cell lines after phagocytosis of HI *S. aureus*. **(d right panel)** Data are presented as a pool of three experiments (mean ± s.e.m). **(a-h)** Data are representative of three independent experiments * p<0.01, **p<0.001 by Student's t-test.

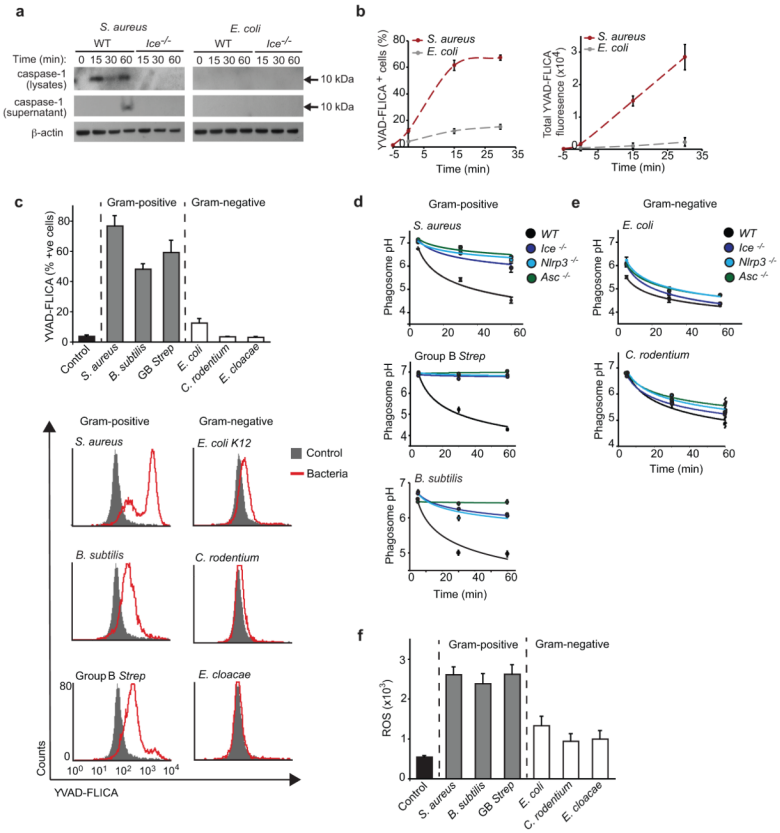

Figure 6. The NLRP3 inflammasome and caspase-1 regulate the pH of phagosomes containing Gram-positive but not Gram-negative bacteria

a, Kinetics of caspase-1 activation in response to live *S. aureus* (MOI: 100) and *E. coli* (MOI: 100) was determined in WT and *Ice*$^{-/-}$ macrophage cell lines by immunoblot of Caspase-1 p10 in total cell lysates or cell supernatants. **b**, Kinetics of caspase-1 activation in response to *S. aureus* (red) *and E. coli* (grey) in BMDM was measured by flow cytometry (MOI: 50). **c**, YVAD-FLICA activity induced by uptake of live Gram-positive and Gram-negative bacteria (MOI: 50). **Upper panel**, Total YVAD-FLICA fluorescence; **lower panel,** flow cytometry histograms. FLICA was added at 15 min bacterial post-internalization for 1h. **d-e** Acidification of HI Gram-positive (**d**) and Gram-negative (**e**) bacteria-containing phagosomes in WT, *Ice*$^{-/-}$, *Nlrp3*$^{-/-}$ and *Asc*$^{-/-}$ BM macrophage cell lines. NLRP3 inflammasome components (Nlrp3, Asc and caspase-1) are shown in green and blue. **f**, Total cellular ROS (H2DCFDA) induced by uptake of live Gram-positive or Gram-negative (MOI: 50) bacteria. ROS was measured at 15 minutes post-internalization. Data are representative of three independent experiments.

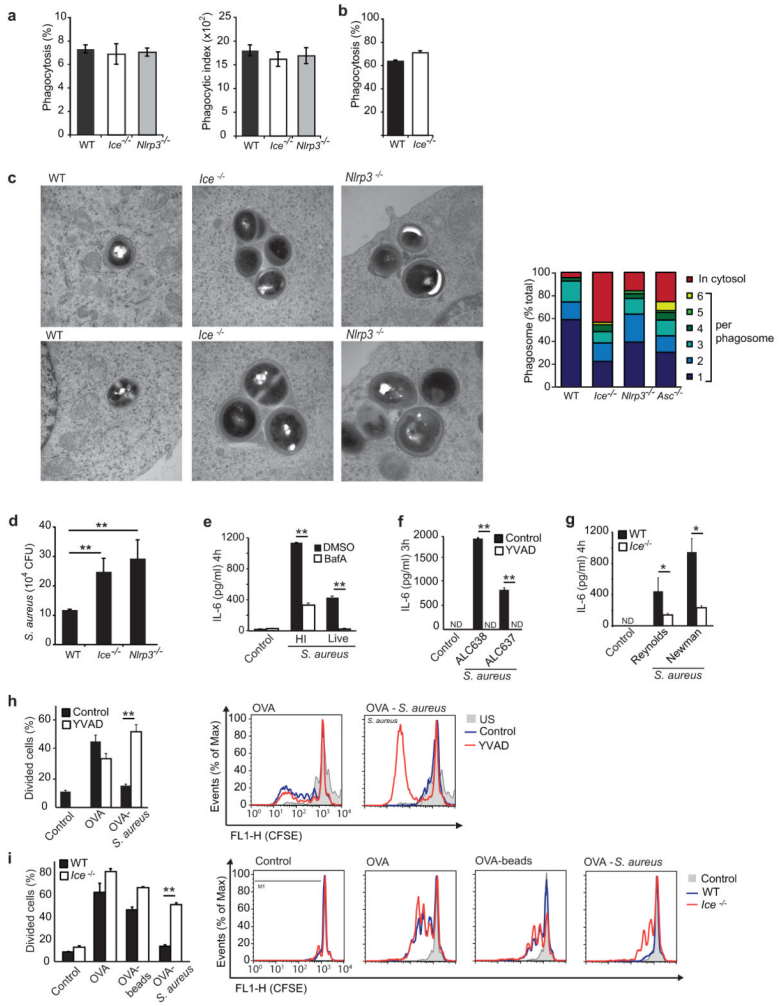

Figure 7. The impact of caspase-1 on the function of phagosomes

a-b, Quantification of bacterial uptake in WT and inflammasome deficient macrophage cell lines at low and high MOIs. **a,** Percentage of phagocytic cells (left) and phagocytic index (MFI of *S. aureus* positive cells) (right) of WT (black bar), *Ice*$^{-/-}$ (white bar) and *Nlrp3*$^{-/-}$ (grey bar) macrophages treated with HI Alexa 647 labeled-*S. aureus* (MOI: 2) for 60 minutes. Mean +/-sem, n=3. **b,** Phagocytosis of WT (black bar) and *Ice*$^{-/-}$ (white bar) macrophages treated with HI Alexa 647 labeled-*S. aureus* (MOI: 25) for 60 minutes. Mean +/-sd of one representative experiment. The percentage of cells that internalized *S. aureus* and the MFI were determined by flow cytometry. **c**, **left panels,** Transmission electron microscopy of live *S. aureus* in WT, *Ice*$^{-/-}$ and *Nlrp3*$^{-/-}$ BM macrophage cell lines 8 hours after infection. **Right panels**, the subcellular localization and number of intra-vacuolar *S. aureus* was quantified by counting. Red, cytosolic bacteria, Other colours correspond to different numbers of intra-vacuolar bacteria in each phagosome. **d**, *S. aureus* (MOI: 5) survival in WT, *Ice*$^{-/-}$ and *Nlrp3*$^{-/-}$ BMDM was determined by gentamicin protection assays 20 hours after infection. **e-g,** IL-6 production by peritoneal macrophages (**e, f**) and BMDM (**g**) after *S. aureus* infection (MOI: 10). Black bars in **e-g** are control and white bars are **e**, Bafilomycin A (100 nM); **f**, YVAD (100 μM); **g**, *Ice*$^{-/-}$. **h-i** Antigen cross-presentation of ovalbumin (OVA) to CD8^{+} OT-I T cells by (**h**) BM macrophages, control (black bars) or pretreated with YVAD (100 μM) (white bars), internalized soluble OVA or OVA conjugated to HI *S. aureus* (MOI: 10) and by (**i**) WT (black bars) and *Ice*$^{-/-}$ (white

bars) BM macrophage cell lines, internalized soluble OVA or OVA conjugated to beads (10 beads/ cell) or HI *S. aureus* (MOI:10). Left panels % divided $CD8^+$ T cells, right, FACS histograms. **(a,b e-i)** Data are representative of three independent experiments (mean ± s.d). **(c)** Data is representative of two independent experiments **(d)** Data are presented as a pool of three experiments (mean ± s.e.m), * $p<0.01$, ** $p<0.001$ by Student's t-test.